

See discussions, stats, and author profiles for this publication at: <https://www.researchgate.net/publication/274095629>

# Discovery of potent and selective urea-based ROCK inhibitors: Exploring the inhibitor's potency and ROCK2/PKA selectivity by 3D-QSAR, molecular docking and molecular dynamics simul...

ARTICLE *in* BIOORGANIC & MEDICINAL CHEMISTRY · MARCH 2015

Impact Factor: 2.79 · DOI: 10.1016/j.bmc.2015.03.047

---

READS

56

## 8 AUTHORS, INCLUDING:



Yangbo Feng

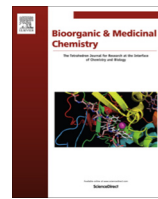
The Scripps Research Institute, Florida

56 PUBLICATIONS 1,173 CITATIONS

SEE PROFILE



Contents lists available at ScienceDirect



# Discovery of potent and selective urea-based ROCK inhibitors: Exploring the inhibitor's potency and ROCK2/PKA selectivity by 3D-QSAR, molecular docking and molecular dynamics simulations

Ding Mei <sup>a</sup>, Yan Yin <sup>a,b,\*</sup>, Fanhong Wu <sup>a</sup>, Jiaxing Cui <sup>a</sup>, Hong Zhou <sup>a</sup>, Guofeng Sun <sup>a</sup>, Yu Jiang <sup>a</sup>, Yangbo Feng <sup>c,\*</sup>

<sup>a</sup> School of Chemical and Environmental Engineering, Shanghai Institute of Technology, 100 Hai Quan Rd., Shanghai 201418, PR China

<sup>b</sup> Key Laboratory of Synthetic Chemistry of Natural Substances, Shanghai Institute of Organic Chemistry, Chinese Academy of Sciences, 345 Ling Ling Rd., Shanghai 200032, PR China

<sup>c</sup> Medicinal Chemistry, Translational Research Institute, The Scripps Research Institute, Florida, Jupiter, FL 33458, USA

## ARTICLE INFO

## Article history:

Received 2 February 2015

Revised 16 March 2015

Accepted 17 March 2015

Available online xxxx

## Keywords:

ROCK inhibitors

ROCK/PKA selectivity

3D-QSAR

Molecular docking

Molecular dynamics simulations

## ABSTRACT

An activity model and a selectivity model from 3D-QSAR studies were established by CoMFA and CoMSIA to explore the SAR. Then docking was used to study the binding modes between ligand and kinases (ROCK2 and PKA), and the molecular docking results were further validated by MD simulations. Computational results suggested that substitution containing positive charge attached to the middle phenyl ring, or electropositive group in urea linker was favored for both activity and ROCK2/PKA selectivity. Finally, three compounds were designed, and biological evaluation demonstrated that these molecular models were effective for guiding the design of potent and selective ROCK inhibitors.

© 2015 Elsevier Ltd. All rights reserved.

## 1. Introduction

Rho-associated coiled-coil protein kinase (ROCK), a serine/threonine protein kinase, is one of the downstream effectors of the small GTPase Rho A and belongs to the AGC family.<sup>1</sup> To date, two isoforms were identified as ROCK1 and ROCK2. Accumulating evidence suggests that ROCK plays essential roles in various cellular functions, such as stress fiber formation, focal adhesion formation, cell aggregation, cell morphology, cytokinesis, cell migration, cell proliferation and apoptosis.<sup>2–4</sup> ROCK inhibitors have been considered to provide a pharmacological strategy for preventing and treating multiple sclerosis, pulmonary hypertension, glaucoma, cardiovascular diseases, erectile dysfunction, and cancer.<sup>5,6</sup> So far, this potential has only been realized by one clinically approved inhibitor (fasudil, marketed in Japan for cerebral vasospasm) although thousands of ROCK inhibitors with diverse structures were developed.<sup>7</sup>

Although the potency of ROCK inhibitors was explored by a series of computational studies including molecular docking, 3D-QSAR analysis, molecular dynamics simulation and free energy

calculations,<sup>8–10</sup> but seldom were focused on the selectivity. In fact, most ROCK inhibitors presented non-ignorable cross-activity against closely related AGC kinases.<sup>11</sup> Through the X-ray crystal structure of ATP-competitive inhibitors bound to ROCK1, Jacobs suggested that interactions with a single residue in the active site (Ala<sup>215</sup> in ROCK1 and Thr<sup>183</sup> in PKA) determined the relative selectivity of Y-27632, fasudil and H-1152P, and hydroxyfasudil may be selective for ROCK over PKA through a reversed binding orientation.<sup>12</sup>

We have discovered a lot of ROCK inhibitors through fragment-based drug design.<sup>13–21</sup> In this work, we plan to reveal the structural and chemical properties that favor ROCK inhibition activity and selectivity through molecular modeling based on the data set collected from our previous publications.<sup>20,21</sup> 3D-QSAR studies including comparative molecular field analyses (CoMFA)<sup>22</sup> and comparative molecular similarity indices analyses (CoMSIA)<sup>23,24</sup> were applied to obtain insights into key structural factors that affect the inhibitory activity and selectivity of ROCK inhibitors. To validate the 3D-QSAR models and to further explore the origin of the selectivity at the amino acid residue level, molecular dockings followed by molecular dynamics simulations was conducted. Finally, the residue which introduced ligand potency and ROCK2/PKA selectivity was discovered and further validated by chemical synthesis and biological evaluation. Herein, the computer-aided

\* Corresponding authors. Tel.: +86 21 60877220; fax: +86 21 60877231 (Y. Yin), tel.: +1 561 2282201; fax: +1 561 2282201 (Y. Feng).

E-mail addresses: [yinyan@sjtu.edu.cn](mailto:yinyan@sjtu.edu.cn) (Y. Yin), [yfeng@scripps.edu](mailto:yfeng@scripps.edu) (Y. Feng).

drug design of highly potent and selective ROCK inhibitors will be described in detail, and the synthetic procedures and structural characterization of the newly designed compounds will also be reported along with the biological experimental protocols.

## 2. Result and discussion

### 2.1. Date set

The urea-based ROCK inhibitors involved in this study were taken from two publications,<sup>20,21</sup> and the chemical structures and IC<sub>50</sub> values against ROCK2 and PKA were listed in Table 1. A total of 54 compounds with ROCK2 IC<sub>50</sub> values were collected to establish activity models and a total of 42 compounds with ROCK2 and PKA IC<sub>50</sub> values were collected to construct selectivity models. These compounds were sorted into training set and test set randomly: 39 into training set and 15 into test set in activity models, 31 into training set and 11 into test set in selectivity models.

### 2.2. CoMFA and CoMSIA statistical results

The statistical results for the final CoMFA and CoMSIA models were summarized in Table 2. When the cross-validated correlation coefficient ( $q^2$ ) after leave-one-out procedure is  $>0.5$ , a model is reliable and predictive.<sup>25,26</sup> In this study, the  $q^2$  values of all models were more than 0.5 ( $q^2 = 0.533$  in CoMFA activity model, 0.538 in CoMSIA activity model, 0.549 in CoMFA selectivity model, and 0.534 in CoMSIA selectivity model, respectively), and the correlation coefficient ( $R^2$ ) values were close to 1 ( $R^2 = 0.979$  in CoMFA activity model, 0.998 in CoMSIA activity model, 0.994 in CoMFA selectivity model, and 0.998 in CoMSIA selectivity model, respectively). In contribution, steric field contributed 68.2%, 20.7%, 61.2%, and 18.4% in CoMFA activity model, CoMSIA activity model, CoMFA selectivity model, and CoMSIA selectivity model, respectively. Electrostatic field contributed 31.8%, 28.0%, 33.8%, and 29.3% in CoMFA activity model, CoMSIA activity model, CoMFA selectivity model, and CoMSIA selectivity model, respectively. Steric field was the major contribution for these 3D-QSAR models.

The experimental and predicted activities of ROCK inhibitors by activity models and selectivity models were listed in Table 3. The residual range ΔpIC<sub>50</sub><sub>residual</sub> ( $\Delta pIC_{50\text{residual}} = pIC_{50\text{pred}} - pIC_{50\text{actual}}$ ) was 0.001 to 2.152 in activity models, and the residual range ΔΔpIC<sub>50</sub><sub>residual</sub> ( $\Delta\Delta pIC_{50\text{residual}} = \Delta pIC_{50\text{pred}} - \Delta pIC_{50\text{actual}}$ ) was 0.000 to 1.870 in selectivity models.

Compounds **2**, **4**, and **47** in activity models and **11** and **30** in selectivity models were considered as outliers and were neglected in the plots of predicted values against experimental values for their residual values exceeded one logarithm unit.<sup>27</sup> The plots of the predicted pIC<sub>50</sub> values versus the experimental ones for CoMFA/CoMSIA analysis were shown in Figure 1. Most points were well distributed along the line Y = X suggested that the quality of the 3D-QSAR models were good.

### 2.3. Contour maps of CoMFA and CoMSIA models

For the convenience of analysis, urea-based ROCK inhibitors were divided into three regions: region I, the terminal phenyl ring; region II, the urea linker; region III, the central phenyl ring (Fig. 2). Since inhibitor **42** was one of the most active compounds and compound **63** was the most selective compound among these chosen compounds, they were used as the reference compounds in activity models and selectivity models, respectively. The 3D contour maps of CoMFA models and CoMSIA models were shown in Figures 3–5.

### 2.3.1. Contour map in region I

As shown in the steric field of CoMFA and CoMSIA activity models, region I was wrapped by a bulky green contour indicating that this region was very important for the activity of ROCK inhibitors, which was in agreement with previous results that compounds without a bulky aromatic group in this region had much lower ROCK inhibitory activities<sup>13</sup> (Fig. 3a and b). In the steric field of CoMFA selectivity model, there were a yellow contour at the 2-position and a green contour at the 3-position of the terminal phenyl ring, which suggested that substitutions at the 3-position were preferred for selectivity than at the 2-position ( $\Delta pIC_{50\text{Actual}} = 2.644$  for **30** with methoxyl group at the 3-position,  $\Delta pIC_{50\text{Actual}} = 1.513$  for **1** without substitutions,  $\Delta pIC_{50\text{Actual}} = 1.401$  for **26** with methoxyl group at the 2-position, Fig. 3c).

Electrostatic contour maps were shown in Figure 4. In the activity models there were red contours at the 3-positions of the phenyl ring, which suggested that at this position electronegative substituent such as, halogen, sulfur, and alkoxy groups was favored for inhibitory activity. For example, inhibitors **4**, **5** and **6** bearing electronegative groups expressed higher activities than **26** (without a substitution) or **3** which had a electropositive substitution at the 3-position (3 nM for **4**, 17 nM for **5**, and 3 nM for **6**, vs 18 nM for **26** and 33 nM for **3**).

The hydrophobic and H-bond donor/acceptor contour maps of CoMSIA models were shown in Figure 5. The existence of large yellow contours indicated that introduction of hydrophobic substitutions in this region would benefit both inhibitory activity and selectivity (Fig. 5a and b). In the H-bond donor/receptor contour maps of CoMSIA selectivity model, the presence of a cyan contour around the 3-position of the terminal phenyl ring indicated that addition of a hydrogen bond donor at the 3-position improved selectivity of ROCK2 over PKA. For example, compound **30** (with an OCH<sub>3</sub> group at the 3-position) showed higher ROCK2/PKA selectivity than **26** which had no any substitutions ( $\Delta pIC_{50\text{Actual}} = 2.644$  for **30** vs 1.513 for **26**, Fig. 5d).

### 2.3.2. Contour map in region II

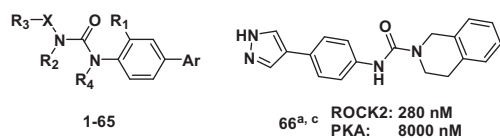
The exhibition of yellow contours around the urea linker region suggested that bulk groups on this area were disfavored (Fig. 3a–c). For example, compounds **50–55** (IC<sub>50</sub> > 1 nM,  $\Delta pIC_{50\text{Actual}} < 3$ ), which had long and bulky substitutions, expressed lower ROCK2 potency and selectivity against PKA compared to compounds **42** and **43** which had small substitutions (IC<sub>50</sub> ≤ 1 nM,  $\Delta pIC_{50\text{Actual}} > 3$ ). Compared the inhibitory activity of compounds **26** with **38–41**, the similar information was obtained (IC<sub>50</sub> = 18 nM for **26**, 87 nM for **38**, 611 nM for **39**, 2984 nM for **40**, 3324 nM for **41**).

In the electrostatic field of activity and selectivity models, there were blue contours, which suggested that electropositive groups in region II were favored for both ROCK2 potency and selectivity against PKA (Fig. 4a–d). For example, compound **43** (with an ethyl group) expressed better potency and selectivity than compounds **46**, **47**, **49**, **50**, and **51** which all had substitutions containing electronegative groups (IC<sub>50</sub> = 1 nM,  $\Delta pIC_{50\text{Actual}} = 3.699$  for **43** vs IC<sub>50</sub> = 1 nM,  $\Delta pIC_{50\text{Actual}} = 3.475$  for **46**; IC<sub>50</sub> = 17 nM,  $\Delta pIC_{50\text{Actual}} = 2.792$  for **47**; IC<sub>50</sub> = 1 nM,  $\Delta pIC_{50\text{Actual}} = 2.659$  for **49**; IC<sub>50</sub> = 3 nM,  $\Delta pIC_{50\text{Actual}} = 2.256$  for **50**; IC<sub>50</sub> = 5 nM,  $\Delta pIC_{50\text{Actual}} = 1.659$  for **51**).

In the hydrophobic contour map of CoMSIA models, there was a huge white contour around this area indicating that hydrophobic groups on this position were disfavored for both ROCK2 potency and selectivity over PKA (Fig. 5a and b). In the H-bond donor/receptor contour maps of selectivity CoMSIA model, there were cyan contours, which meant that addition of an H-bond donor was favored for selectivity. For example, **46** (with –CH<sub>2</sub>CH<sub>2</sub>OH group) showed better selectivity than **30** ( $\Delta pIC_{50\text{Actual}} = 3.475$  for **46** vs  $\Delta pIC_{50\text{Actual}} = 2.644$  for **30**, Fig. 5d).

**Table 1**

**Table 1**  
The structures and experimental IC<sub>50</sub> values of urea-based ROCK inhibitors



| Compd             | Ar | R <sub>1</sub>                    | R <sub>2</sub>  | R <sub>3</sub> | R <sub>4</sub> | X               | ROCK2 IC <sub>50</sub> (nM) | PKA IC <sub>50</sub> (nM) |
|-------------------|----|-----------------------------------|-----------------|----------------|----------------|-----------------|-----------------------------|---------------------------|
| 1 <sup>a,c</sup>  |    | H                                 | H               |                | H              | CH <sub>2</sub> | 26                          | 654                       |
| 2 <sup>b</sup>    |    | H                                 | H               |                | H              | CH <sub>2</sub> | 2750                        | ND                        |
| 3 <sup>a,d</sup>  |    | H                                 | H               |                | H              | CH <sub>2</sub> | 33                          | 2630                      |
| 4 <sup>b,c</sup>  |    | H                                 | H               |                | H              | CH <sub>2</sub> | 3                           | 405                       |
| 5 <sup>a,c</sup>  |    | H                                 | H               |                | H              | CH <sub>2</sub> | 17                          | 454                       |
| 6 <sup>b,c</sup>  |    | H                                 | H               |                | H              | CH <sub>2</sub> | 3                           | 322                       |
| 7 <sup>a,c</sup>  |    | H                                 | H               |                | H              | CH <sub>2</sub> | 2                           | 816                       |
| 8 <sup>a,c</sup>  |    | H                                 | H               |                | H              | CH <sub>2</sub> | 5                           | 2304                      |
| 9 <sup>a,d</sup>  |    | H                                 | H               |                | H              | CH <sub>2</sub> | 13                          | 1031                      |
| 10 <sup>a,c</sup> |    | H                                 | H               |                | H              | CH <sub>2</sub> | 44                          | 5142                      |
| 11 <sup>a,d</sup> |    | H                                 | H               |                | H              | CH <sub>2</sub> | 188                         | 744                       |
| 12                |    | -N(CH <sub>3</sub> ) <sub>2</sub> | H               |                | H              | CH <sub>2</sub> | <1                          | 38                        |
| 13                |    | -OCH <sub>3</sub>                 | H               |                | H              | CH <sub>2</sub> | <1                          | 163                       |
| 14                |    | -Cl                               | H               |                | H              | CH <sub>2</sub> | <1                          | 313                       |
| 15                |    | -F                                | H               |                | H              | CH <sub>2</sub> | <1                          | 1821                      |
| 16                |    |                                   | H               |                | H              | CH <sub>2</sub> | <1                          | 3900                      |
| 17                |    |                                   | H               |                | H              | CH <sub>2</sub> | <1                          | 2727                      |
| 18                |    |                                   | H               |                | H              | CH <sub>2</sub> | <1                          | 3573                      |
| 19                |    |                                   | CH <sub>3</sub> |                | H              | CH <sub>2</sub> | <1                          | 5225                      |
| 20                |    |                                   | CH <sub>3</sub> |                | H              | CH <sub>2</sub> | <1                          | >20,000                   |
| 21 <sup>a,c</sup> |    |                                   | CH <sub>3</sub> |                | H              | CH <sub>2</sub> | 8                           | 4618                      |

(continued on next page)

**Table 1** (continued)

| Compd             | Ar | R <sub>1</sub> | R <sub>2</sub>                | R <sub>3</sub> | R <sub>4</sub>  | X                               | ROCK2 IC <sub>50</sub> (nM) | PKA IC <sub>50</sub> (nM) |
|-------------------|----|----------------|-------------------------------|----------------|-----------------|---------------------------------|-----------------------------|---------------------------|
| 22 <sup>a</sup>   |    |                | C <sub>2</sub> H <sub>5</sub> |                | H               | CH <sub>2</sub>                 | 3                           | >20,000                   |
| 23                |    |                | C <sub>2</sub> H <sub>5</sub> |                | H               | CH <sub>2</sub>                 | <1                          | 18,090                    |
| 24 <sup>a,c</sup> |    |                | C <sub>2</sub> H <sub>5</sub> |                | H               | CH <sub>2</sub>                 | 6                           | 5004                      |
| 25 <sup>b</sup>   |    | H              | H                             |                | H               | -NR                             | 304                         | >20,000                   |
| 26 <sup>a,d</sup> |    | H              | H                             |                | H               | CH <sub>2</sub>                 | 18                          | 590                       |
| 27 <sup>a,d</sup> |    | H              | H                             |                | H               | CH <sub>2</sub> CH <sub>2</sub> | 88                          | 3098                      |
| 28 <sup>a</sup>   |    | H              | H                             |                | H               |                                 | 1017                        | >20,000                   |
| 29 <sup>a</sup>   |    | H              | H                             |                | H               | CH <sub>2</sub>                 | 751                         | >20,000                   |
| 30 <sup>a,d</sup> |    | H              | H                             |                | H               | CH <sub>2</sub>                 | 2                           | 882                       |
| 31 <sup>a</sup>   |    | H              | H                             |                | H               | CH <sub>2</sub>                 | 253                         | >20,000                   |
| 32 <sup>a,c</sup> |    | H              | H                             |                | H               | CH <sub>2</sub>                 | 331                         | 11,170                    |
| 33 <sup>a</sup>   |    | H              | H                             |                | H               | CH <sub>2</sub>                 | 570                         | >20,000                   |
| 34 <sup>b,c</sup> |    | H              | H                             |                | H               | CH <sub>2</sub>                 | 924                         | 13,480                    |
| 35 <sup>a</sup>   |    | H              | H                             |                | H               | CH <sub>2</sub>                 | 425                         | >20,000                   |
| 36 <sup>a</sup>   |    | H              | H                             |                | H               | CH <sub>2</sub>                 | 281                         | >20,000                   |
| 37 <sup>b,c</sup> |    | H              | H                             |                | H               | CH <sub>2</sub>                 | 357                         | 518                       |
| 38 <sup>a</sup>   |    | H              | H                             | H              | CH <sub>3</sub> | CH <sub>2</sub>                 | 87                          | >20,000                   |
| 39 <sup>a</sup>   |    | H              | H                             | H              |                 | CH <sub>2</sub>                 | 611                         | >20,000                   |
| 40 <sup>a,c</sup> |    | H              | H                             | H              |                 | CH <sub>2</sub>                 | 2984                        | 4196                      |
| 41 <sup>a,c</sup> |    | H              | H                             | H              |                 | CH <sub>2</sub>                 | 3324                        | 12,010                    |
| 42 <sup>a,c</sup> |    | H              | CH <sub>3</sub>               |                | H               | CH <sub>2</sub>                 | 1                           | 1809                      |

**Table 1** (continued)

| Compd             | Ar | R <sub>1</sub> | R <sub>2</sub>                  | R <sub>3</sub> | R <sub>4</sub> | X               | ROCK2 IC <sub>50</sub> (nM) | PKA IC <sub>50</sub> (nM) |
|-------------------|----|----------------|---------------------------------|----------------|----------------|-----------------|-----------------------------|---------------------------|
| 43 <sup>a,c</sup> |    | H              | CH <sub>2</sub> CH <sub>3</sub> |                | H              | CH <sub>2</sub> | 1                           | 4667                      |
| 44 <sup>a,d</sup> |    | H              |                                 |                | H              | CH <sub>2</sub> | 1                           | 1705                      |
| 45 <sup>b,c</sup> |    | H              |                                 |                | H              | CH <sub>2</sub> | 3                           | 18,450                    |
| 46 <sup>a,c</sup> |    | H              |                                 |                | H              | CH <sub>2</sub> | 1                           | 2988                      |
| 47 <sup>b,c</sup> |    | H              |                                 |                | H              | CH <sub>2</sub> | 17                          | 10,530                    |
| 48                |    | H              |                                 |                | H              | CH <sub>2</sub> | <1                          | 72                        |
| 49 <sup>a,d</sup> |    | H              |                                 |                | H              | CH <sub>2</sub> | 1                           | 456                       |
| 50 <sup>a,c</sup> |    | H              |                                 |                | H              | CH <sub>2</sub> | 3                           | 541                       |
| 51 <sup>b,c</sup> |    | H              |                                 |                | H              | CH <sub>2</sub> | 5                           | 228                       |
| 52 <sup>a,c</sup> |    | H              |                                 |                | H              | CH <sub>2</sub> | 13                          | 3823                      |
| 53 <sup>a,d</sup> |    | H              |                                 |                | H              | CH <sub>2</sub> | 4                           | 724                       |
| 54 <sup>b,c</sup> |    | H              |                                 |                | H              | CH <sub>2</sub> | 5                           | 338                       |
| 55 <sup>a,c</sup> |    | H              |                                 |                | H              | CH <sub>2</sub> | 4                           | 822                       |
| 56 <sup>b,d</sup> |    | H              |                                 |                | H              | CH <sub>2</sub> | 12                          | 610                       |
| 57 <sup>b,c</sup> |    | F              |                                 |                | H              | CH <sub>2</sub> | 14                          | 1016                      |

(continued on next page)

**Table 1 (continued)**

| Compd             | Ar  | R <sub>1</sub>  | R <sub>2</sub>  | R <sub>3</sub>   | R <sub>4</sub> | X   | ROCK2 IC <sub>50</sub> (nM) | PKA IC <sub>50</sub> (nM) |
|-------------------|---|---|---|--|----------------|---|-----------------------------|---------------------------|
| 58 <sup>b,c</sup> |  | H   | H   |   | H              |  | 2                           | 4871                      |
| 59 <sup>a,c</sup> |  | H   | H   |   | H              |  | 2                           | 580                       |
| 60 <sup>b,d</sup> |  | H   | H   |   | H              |  | 1                           | 438                       |
| 61 <sup>a,c</sup> |  | H   | H   |   | H              |  | 2                           | 389                       |
| 62 <sup>b,c</sup> |  | H   | H   |   | H              |  | 2                           | 238                       |
| 63 <sup>a,c</sup> |  |  | -CH <sub>2</sub> CH <sub>3</sub>  |   | H              | CH <sub>2</sub>   | 1                           | 6700                      |
| 64                |  |  |  |  | H              | CH <sub>2</sub>   | <1                          | 615                       |
| 65 <sup>a</sup>   |  |  |  |  | H              | CH <sub>2</sub>   | 170                         | N/R                       |

<sup>a</sup> Training set of activity model.<sup>b</sup> Test set of activity model.<sup>c</sup> Training set of selectivity model.<sup>d</sup> Test set of selectivity model.**Table 2**  
Statistical results of the activity models and selectivity models

| Statistical parameters | Activity models |          | Selectivity models |         |
|------------------------|-----------------|----------|--------------------|---------|
|                        | CoMFA           | CoMSIA   | CoMFA              | CoMSIA  |
| <i>q</i> <sup>2</sup>  | 0.533           | 0.538    | 0.549              | 0.534   |
| ONC                    | 5               | 9        | 10                 | 12      |
| <i>R</i> <sup>2</sup>  | 0.979           | 0.998    | 0.994              | 0.998   |
| SEE                    | 0.170           | 0.056    | 0.093              | 0.058   |
| <i>F</i>               | 315.284         | 1645.181 | 323.365            | 693.392 |
| <i>Contribution</i>    |                 |          |                    |         |
| <i>S</i>               | 0.682           | 0.207    | 0.612              | 0.184   |
| <i>E</i>               | 0.318           | 0.280    | 0.338              | 0.293   |
| <i>H</i>               | —               | 0.283    | —                  | 0.254   |
| <i>D</i>               | —               | 0.140    | —                  | 0.130   |
| <i>A</i>               | —               | 0.090    | —                  | 0.140   |

### 2.3.3. Contour map in region III

In region III, there were green contours in the steric field and blue contours in the electrostatic field, which indicated that substitutions containing a positive charge attached to the phenyl ring would increase the potency and selectivity of ROCK inhibitors (Fig. 3a–c, and 4a–c). For example, compound **16**, which had a substitution containing a protonated tertiary amine attached to the phenyl ring, had higher ROCK potency and selectivity than compound **30** which had no any substitutions on the phenyl ring ( $IC_{50} < 1$  nM,  $\Delta pIC_{50}\text{Actual} > 3.454$  for **16** vs  $IC_{50} = 2$  nM,  $\Delta pIC_{50}\text{Actual} = 2.644$  for **30**).

### 2.4. Docking results

3D-QSAR studies demonstrated that substitution containing positive charge attached to the phenyl ring was favored for both activity and selectivity (Fig. 2). Both compounds **16** and **12** had a substitution containing positive charge attached to the phenyl ring,

but the PKA inhibitory activities between them were quite different. So we further explored the high selectivity of this series of urea-based ROCK inhibitors from amino acid level through molecular docking.

Docking protocol is widely used to explore the binding affinity.<sup>28</sup> Previous docking studies demonstrated that both H-bonding and hydrophobic interactions between ligand **16** and ROCK2 protein contributed to the high potency of these urea-based ROCK2 inhibitors, and the key residues for H-bonding interactions were Glu170, Met172, Lys121, and Asp176 (Fig. 6a).<sup>21</sup> H-bonding interactions between ligand and residues Val123, Glu121, Lys72, and Asn171/Asp184 were the key interactions for PKA inhibitory activity.<sup>29</sup> Kwang-Seok Oh et al. reported that interactions from single amino acid residue of active site (Asp176 in ROCK2 and Glu183 in PKA) determined the relative selectivity of ROCK2 over PKA.<sup>30</sup>

Compound **16** ( $IC_{50} < 1$  nM against ROCK2 and  $IC_{50} = 3900$  nM against PKA) and **12** ( $IC_{50} < 1$  nM against ROCK2 and  $IC_{50} = 38$  nM against PKA) were docking into the catalytic domain of both human ROCK2 and human PKA proteins (Fig. 6). H-bonding interactions with residues Val123, Glu121, Asp184, Asn171, and Thr51 were the key interactions for **16** in PKA (Fig. 7c), and H-bonding interactions with residues Ala123, Glu121, Lys72, and Glu170 were the key interactions for **12** in the active site of PKA (Fig. 6d). A more than 100-fold difference of PKA inhibitory activity between **12** and **16** is highly likely due to the hydrophobic interactions between terminal phenyl ring and PKA in **12**. However, the dimethylaminoethoxy group in central phenyl ring of **16** had disturbed the optimal binding conformation of **16** and caused the terminal phenyl ring leaved the hydrophobic pocket of PKA.

### 2.5. MD simulations results

The MD simulations were carried out for 5 ns to validate the docking accuracy, and the results were shown in Figure 8. The

**Table 3**  
Experimental and predicted activities

| Compd                  | Actual<br>$\text{pIC}_{50}$ | CoMFA                          |  | CoMSIA                         |  | <b>8</b>              | <b>2.633</b> | <b>2.607</b> | −0.056 | 2.659        | −0.004 |  |  |  |  |  |  |  |
|------------------------|-----------------------------|--------------------------------|--|--------------------------------|--|-----------------------|--------------|--------------|--------|--------------|--------|--|--|--|--|--|--|--|
|                        |                             | Predicted<br>$\text{pIC}_{50}$ | Residual <sup>a</sup><br>$\Delta\text{pIC}_{50}$ | Predicted<br>$\text{pIC}_{50}$ | Residual <sup>a</sup><br>$\Delta\text{pIC}_{50}$ |                       |              |              |        |              |        |  |  |  |  |  |  |  |
|                        |                             |                                |  |                                |  |                       |              |              |        |              |        |  |  |  |  |  |  |  |
| <i>Activity models</i> |                             |                                |  |                                |  |                       |              |              |        |              |        |  |  |  |  |  |  |  |
| <i>Training set</i>    |                             |                                |  |                                |  |                       |              |              |        |              |        |  |  |  |  |  |  |  |
| <b>1</b>               | 7.585                       | 7.762                          | 0.177  | 7.51                           | −0.075   | <b>10</b>             | <b>2.068</b> | <b>2.105</b> | 0.037  | <b>2.07</b>  | 0.002  |  |  |  |  |  |  |  |
| <b>3</b>               | 7.481                       | 7.453                          | −0.028   | 7.535                          | 0.054  | <b>21</b>             | <b>2.761</b> | <b>2.734</b> | −0.027 | <b>2.774</b> | 0.013  |  |  |  |  |  |  |  |
| <b>5</b>               | 7.77                        | 7.761                          | −0.009   | 7.675                          | −0.095   | <b>24</b>             | <b>2.921</b> | <b>2.935</b> | 0.014  | <b>2.923</b> | 0.002  |  |  |  |  |  |  |  |
| <b>7</b>               | 8.699                       | 8.719                          | 0.02   | 8.738                          | 0.039  | <b>32</b>             | <b>1.528</b> | <b>1.549</b> | 0.021  | <b>1.537</b> | 0.009  |  |  |  |  |  |  |  |
| <b>8</b>               | 8.301                       | 8.119                          | −0.182   | 8.398                          | 0.097  | <b>34</b>             | <b>1.164</b> | <b>1.123</b> | −0.041 | <b>1.127</b> | −0.037 |  |  |  |  |  |  |  |
| <b>9</b>               | 7.886                       | 7.858                          | −0.028   | 7.872                          | 0.014  | <b>37</b>             | <b>0.161</b> | <b>0.179</b> | 0.018  | <b>0.119</b> | −0.042 |  |  |  |  |  |  |  |
| <b>10</b>              | 7.357                       | 7.498                          | 0.141  | 7.369                          | 0.012  | <b>40</b>             | <b>0.148</b> | <b>0.126</b> | −0.022 | <b>0.152</b> | 0.004  |  |  |  |  |  |  |  |
| <b>11</b>              | 6.726                       | 6.946                          | 0.22   | 6.729                          | 0.003  | <b>41</b>             | <b>0.558</b> | <b>0.588</b> | 0.03   | <b>0.571</b> | 0.013  |  |  |  |  |  |  |  |
| <b>21</b>              | 8.097                       | 7.835                          | −0.262   | 8.149                          | −0.052   | <b>42</b>             | <b>3.257</b> | <b>3.216</b> | −0.041 | <b>3.324</b> | 0.067  |  |  |  |  |  |  |  |
| <b>22</b>              | 8.523                       | 8.478                          | −0.045   | 8.522                          | −0.001   | <b>43</b>             | <b>3.669</b> | <b>3.669</b> | 0      | <b>3.593</b> | −0.076 |  |  |  |  |  |  |  |
| <b>24</b>              | 8.222                       | 8.205                          | −0.017   | 8.24                           | −0.018   | <b>45</b>             | <b>3.789</b> | <b>3.805</b> | 0.016  | <b>3.794</b> | 0.005  |  |  |  |  |  |  |  |
| <b>26</b>              | 7.745                       | 7.582                          | −0.163   | 7.736                          | −0.009   | <b>46</b>             | <b>3.475</b> | <b>3.461</b> | −0.014 | <b>3.479</b> | 0.004  |  |  |  |  |  |  |  |
| <b>27</b>              | 7.055                       | 7.042                          | −0.013   | 7.041                          | −0.014   | <b>47</b>             | <b>2.792</b> | <b>2.784</b> | −0.008 | <b>2.782</b> | −0.01  |  |  |  |  |  |  |  |
| <b>28</b>              | 5.993                       | 6.122                          | 0.129  | 5.969                          | 0.024  | <b>48</b>             | <b>2.256</b> | <b>2.202</b> | −0.054 | <b>2.307</b> | 0.051  |  |  |  |  |  |  |  |
| <b>29</b>              | 6.124                       | 6.224                          | 0.1  | 6.12                           | −0.004   | <b>51</b>             | <b>1.659</b> | <b>1.63</b>  | −0.029 | <b>1.675</b> | 0.016  |  |  |  |  |  |  |  |
| <b>30</b>              | 8.699                       | 8.398                          | −0.301   | 8.698                          | −0.001   | <b>52</b>             | <b>2.468</b> | <b>2.53</b>  | 0.062  | <b>2.41</b>  | −0.058 |  |  |  |  |  |  |  |
| <b>31</b>              | 6.597                       | 6.621                          | 0.024  | 6.589                          | −0.008   | <b>54</b>             | <b>1.83</b>  | <b>1.83</b>  | 0      | <b>1.854</b> | 0.024  |  |  |  |  |  |  |  |
| <b>32</b>              | 6.48                        | 6.303                          | −0.177   | 6.354                          | −0.126   | <b>55</b>             | <b>2.313</b> | <b>2.35</b>  | 0.037  | <b>2.317</b> | 0.004  |  |  |  |  |  |  |  |
| <b>33</b>              | 6.244                       | 5.864                          | −0.38  | 6.334                          | 0.09   | <b>57</b>             | <b>1.861</b> | <b>1.872</b> | 0.011  | <b>1.853</b> | −0.008 |  |  |  |  |  |  |  |
| <b>35</b>              | 6.372                       | 6.461                          | 0.089  | 6.397                          | 0.025  | <b>58</b>             | <b>3.387</b> | <b>3.361</b> | −0.026 | <b>3.418</b> | 0.031  |  |  |  |  |  |  |  |
| <b>36</b>              | 6.551                       | 6.535                          | −0.016   | 6.545                          | −0.006   | <b>59</b>             | <b>2.462</b> | <b>2.455</b> | −0.007 | <b>2.484</b> | 0.022  |  |  |  |  |  |  |  |
| <b>38</b>              | 7.06                        | 6.898                          | −0.162   | 6.997                          | −0.063   | <b>61</b>             | <b>2.289</b> | <b>2.31</b>  | 0.021  | <b>2.257</b> | −0.032 |  |  |  |  |  |  |  |
| <b>39</b>              | 6.214                       | 6.283                          | 0.069  | 6.17                           | −0.004   | <b>62</b>             | <b>2.076</b> | <b>2.13</b>  | 0.054  | <b>2.074</b> | −0.002 |  |  |  |  |  |  |  |
| <b>40</b>              | 5.525                       | 5.809                          | 0.284  | 5.595                          | 0.07   | <b>63</b>             | <b>3.826</b> | <b>3.864</b> | 0.038  | <b>3.799</b> | −0.027 |  |  |  |  |  |  |  |
| <b>41</b>              | 5.478                       | 5.654                          | 0.176  | 5.506                          | 0.028  | <b>66</b>             | <b>1.456</b> | <b>1.449</b> | −0.007 | <b>1.46</b>  | 0.004  |  |  |  |  |  |  |  |
| <b>42</b>              | 9                           | 9.152                          | 0.152  | 9.006                          | 0.006  | <i>Test set</i>       |              |              |        |              |        |  |  |  |  |  |  |  |
| <b>43</b>              | 9                           | 9.014                          | 0.014  | 8.99                           | −0.01  | <b>3</b>              | <b>1.901</b> | <b>1.898</b> | −0.003 | <b>1.632</b> | −0.269 |  |  |  |  |  |  |  |
| <b>44</b>              | 9                           | 9.105                          | 0.105  | 9.044                          | 0.044  | <b>9</b>              | <b>1.899</b> | <b>1.828</b> | −0.071 | <b>1.516</b> | −0.383 |  |  |  |  |  |  |  |
| <b>46</b>              | 9                           | 9.016                          | 0.016  | 8.978                          | −0.022   | <b>11<sup>c</sup></b> | <b>0.598</b> | <b>2.018</b> | 1.42   | <b>2.468</b> | 1.87   |  |  |  |  |  |  |  |
| <b>49</b>              | 9                           | 8.823                          | −0.177   | 8.889                          | −0.111   | <b>26</b>             | <b>1.513</b> | <b>2.02</b>  | 0.507  | <b>2.474</b> | 0.961  |  |  |  |  |  |  |  |
| <b>50</b>              | 8.523                       | 8.379                          | −0.144   | 8.577                          | 0.034  | <b>27</b>             | <b>1.546</b> | <b>2.47</b>  | 0.924  | <b>2.522</b> | 0.976  |  |  |  |  |  |  |  |
| <b>52</b>              | 7.886                       | 8.075                          | 0.189  | 7.894                          | 0.008  | <b>30<sup>c</sup></b> | <b>2.644</b> | <b>1.429</b> | −1.215 | <b>1.035</b> | −1.609 |  |  |  |  |  |  |  |
| <b>53</b>              | 8.398                       | 8.534                          | 0.136  | 8.425                          | 0.027  | <b>44</b>             | <b>3.232</b> | <b>3.06</b>  | −0.172 | <b>3.271</b> | 0.039  |  |  |  |  |  |  |  |
| <b>55</b>              | 8.398                       | 8.414                          | 0.016  | 8.373                          | −0.025   | <b>49</b>             | <b>2.659</b> | <b>2.461</b> | −0.198 | <b>2.462</b> | −0.197 |  |  |  |  |  |  |  |
| <b>59</b>              | 8.699                       | 8.559                          | −0.14  | 8.707                          | 0.008  | <b>53</b>             | <b>2.258</b> | <b>2.432</b> | 0.174  | <b>1.985</b> | −0.273 |  |  |  |  |  |  |  |
| <b>61</b>              | 8.699                       | 8.746                          | 0.047  | 8.707                          | 0.008  | <b>56</b>             | <b>1.706</b> | <b>2.527</b> | 0.821  | <b>2.673</b> | 0.967  |  |  |  |  |  |  |  |
| <b>63</b>              | 9                           | 9.298                          | 0.298  | 8.989                          | −0.011   | <b>60</b>             | <b>2.641</b> | <b>2.481</b> | −0.16  | <b>2.75</b>  | 0.109  |  |  |  |  |  |  |  |
| <b>65</b>              | 6.77                        | 6.628                          | −0.142   | 6.786                          | 0.016  |                       |              |              |        |              |        |  |  |  |  |  |  |  |
| <b>66</b>              | 6.553                       | 6.535                          | −0.018   | 6.592                          | −0.039   |                       |              |              |        |              |        |  |  |  |  |  |  |  |
| <i>Test set</i>        |                             |                                |  |                                |  |                       |              |              |        |              |        |  |  |  |  |  |  |  |
| <b>2<sup>b</sup></b>   | <b>5.561</b>                | <b>7.713</b>                   | <b>2.152</b>                                     | <b>7.229</b>                   | <b>1.668</b>                                     |                       |              |              |        |              |        |  |  |  |  |  |  |  |
| <b>4<sup>b</sup></b>   | <b>8.523</b>                | <b>7.53</b>                    | <b>−0.993</b>                                    | <b>7.374</b>                   | <b>−1.149</b>                                    |                       |              |              |        |              |        |  |  |  |  |  |  |  |
| <b>6</b>               | <b>8.523</b>                | <b>7.803</b>                   | <b>−0.72</b>                                     | <b>7.621</b>                   | <b>−0.902</b>                                    |                       |              |              |        |              |        |  |  |  |  |  |  |  |
| <b>25</b>              | <b>6.517</b>                | <b>7.151</b>                   | <b>0.634</b>                                     | <b>7.447</b>                   | <b>0.93</b>                                      |                       |              |              |        |              |        |  |  |  |  |  |  |  |
| <b>34</b>              | <b>6.034</b>                | <b>6.319</b>                   | <b>0.285</b>                                     | <b>6.503</b>                   | <b>0.469</b>                                     |                       |              |              |        |              |        |  |  |  |  |  |  |  |
| <b>37</b>              | <b>6.447</b>                | <b>7.317</b>                   | <b>0.87</b>                                      | <b>6.785</b>                   | <b>0.338</b>                                     |                       |              |              |        |              |        |  |  |  |  |  |  |  |
| <b>45</b>              | <b>8.523</b>                | <b>8.869</b>                   | <b>0.346</b>                                     | <b>8.834</b>                   | <b>0.311</b>                                     |                       |              |              |        |              |        |  |  |  |  |  |  |  |
| <b>47<sup>b</sup></b>  | <b>7.77</b>                 | <b>8.543</b>                   | <b>0.773</b>                                     | <b>8.872</b>                   | <b>1.102</b>                                     |                       |              |              |        |              |        |  |  |  |  |  |  |  |
| <b>51</b>              | <b>8.301</b>                | <b>8.595</b>                   | <b>0.294</b>                                     | <b>8.497</b>                   | <b>0.196</b>                                     |                       |              |              |        |              |        |  |  |  |  |  |  |  |
| <b>54</b>              | <b>8.301</b>                | <b>8.326</b>                   | <b>0.025</b>                                     | <b>8.516</b>                   | <b>0.215</b>                                     |                       |              |              |        |              |        |  |  |  |  |  |  |  |
| <b>56</b>              | <b>7.921</b>                | <b>8.780</b>                   | <b>0.859</b>                                     | <b>8.340</b>                   | <b>0.419</b>                                     |                       |              |              |        |              |        |  |  |  |  |  |  |  |
| <b>57</b>              | <b>7.854</b>                | <b>8.652</b>                   | <b>0.798</b>                                     | <b>8.162</b>                   | <b>0.308</b>                                     |                       |              |              |        |              |        |  |  |  |  |  |  |  |
| <b>58</b>              | <b>8.699</b>                | <b>8.508</b>                   | <b>−0.191</b>                                    | <b>8.754</b>                   | <b>0.055</b>                                     |                       |              |              |        |              |        |  |  |  |  |  |  |  |
| <b>60</b>              | <b>9</b>                    | <b>8.423</b>                   | <b>−0.577</b>                                    | <b>8.646</b>                   | <b>−0.354</b>                                    |                       |              |              |        |              |        |  |  |  |  |  |  |  |
| <b>62</b>              | <b>8.699</b>                | <b>7.892</b>                   | <b>−0.807</b>                                    | <b>8.071</b>                   | <b>−0.628</b>                                    |                       |              |              |        |              |        |  |  |  |  |  |  |  |

<sup>a</sup> Residual  $\Delta\text{pIC}_{50\text{residual}} = \text{pIC}_{50\text{pred}} - \text{pIC}_{50\text{actual}}$ .

<sup>b</sup> The outlier compounds.

| Compd                     | Actual <sup>a</sup><br>$\Delta\text{pIC}_{50}$ | CoMFA   |  | CoMSIA  |  | <b>8</b> | <b>2.633</b> | <b>2.607</b> | −0.056 | 2.659 | −0.004 |  |  |  |  |  |  |  |
|---------------------------|--|---|--|---|--|----------|--------------|--------------|--------|-------|--------|--|--|--|--|--|--|--|
|                           |  | Predicted <sup>a</sup><br>$\Delta\text{pIC}_{50}$ | Residual <sup>b</sup><br>$\Delta\Delta\text{pIC}_{50}$ | Predicted <sup>a</sup><br>$\Delta\text{pIC}_{50}$ | Residual <sup>b</sup><br>$\Delta\Delta\text{pIC}_{50}$ |          |              |              |        |       |        |  |  |  |  |  |  |  |
|                           |  |   |  |   |  |          |              |              |        |       |        |  |  |  |  |  |  |  |
| <i>Selectivity models</i> |  |   |  |   |  |          |              |              |        |       |        |  |  |  |  |  |  |  |
| <i>Training set</i>       |  |   |  |   |  |          |              |              |        |       |        |  |  |  |  |  |  |  |
| <b>1</b>                  | <b>1.401</b>                                   | <b>1.342</b>                                      | <b>−0.059</b>  | <b>1.388</b>                                      | <b>−0.013</b>  |          |              |              |        |       |        |  |  |  |  |  |  |  |
| <b>4</b>                  | <b>2.13</b>                                    | <b>2.028</b>                                      | <b>−0.102</b>  | <b>2.139</b>                                      | <b>0.009</b>   |          |              |              |        |       |        |  |  |  |  |  |  |  |
| <b>5</b>                  | <b>1.427</b>                                   | <b>1.737</b>                                      | <b>0.31</b>  | <b>1.577</b>                                      | <b>0.15</b>  |          |              |              |        |       |        |  |  |  |  |  |  |  |
| <b>6</b>                  | <b>2.031</b>                                   | <b>1.838</b>                                      | <b>−0.193</b>  | <b>1.913</b>                                      | <b>−0.118</b>  |          |              |              |        |       |        |  |  |  |  |  |  |  |
| <b>7</b>                  | <b>2.611</b>                                   | <b>2.63</b>                                       | <b>0.019</b>   | <b>2.608</b>                                      | <b>−0.003</b>  |          |              |              |        |       |        |  |  |  |  |  |  |  |

magenta and green structure represent the initial and final protein-ligand complex (**4L6Q–16** complex), respectively. The initial and final structures were in the same binding pocket, and the pharmacophore structure and other structures were basically similar. It could be inferred that the binding pocket and the conformation of the ligand were stable and the docking results were reliable.

## 2.6. Designs of urea-based ROCK inhibitors

Evaluating a model is not only by how well it fits the data, but more importantly by how well it predicts data. Therefore, we tested our models through synthesis and biological evaluation of newly designed ROCK2 inhibitors. From molecular modeling we knew that appropriate substituent in region III and electropositive group in region II were favored for both the activity and selectivity. We thus focused the modification on region III and region II of compound **26** to design potent and selective ROCK inhibitors. As shown in Table 4, compound **D1** had a  $-\text{SCH}_2\text{CH}_2\text{N}(\text{CH}_3)_2$  group and **D2** had a  $-\text{N}(\text{CH}_3)\text{CH}_2\text{CH}_2\text{N}(\text{CH}_3)_2$  group on the central phenyl ring, and **D3** had a  $-\text{CH}(\text{CH}_3)_2$  group on the urea linker. These three compounds were prepared and evaluated for their ROCK2 and PKA potency from biochemical assays and the established 3D-QSAR models (Table 4). Remarkably, the  $\text{IC}_{50}$  values obtained from 3D-QSAR models and biochemical assays were quite similar and within the allowed error range (less than 10 times).<sup>27</sup> Experimental data also showed that compounds **D1**, **D2**, and **D3** had better ROCK2 inhibition and ROCK2/PKA selectivity than lead compound **26** (5.6 nM for **D1**, 8.5 nM for **D2**, 8.0 nM for **D3** vs 18 nM for **26**, and 84-fold selectivity

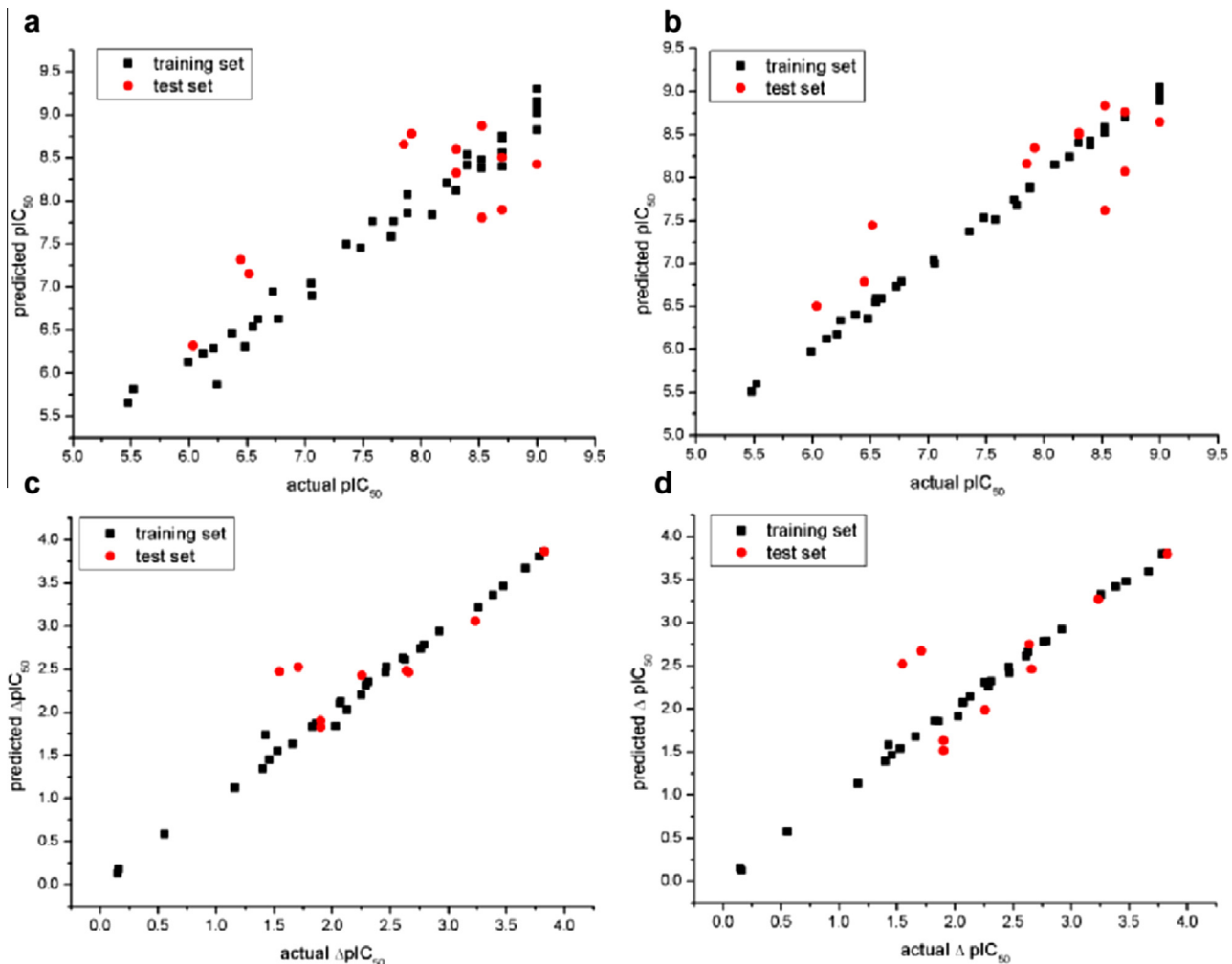


**Figure 1.** Plots of predicted values against experimental values. (a) CoMFA activity model. (b) CoMSIA activity model. (c) CoMFA selectivity model. (d) CoMSIA selectivity model.

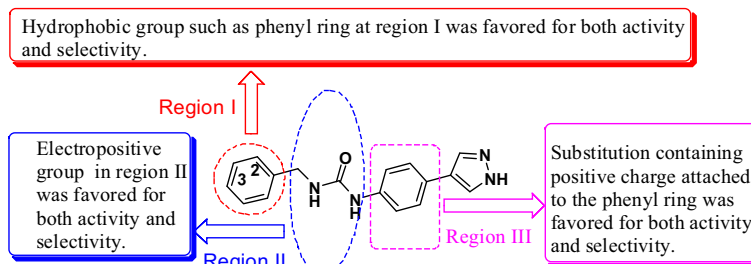


**Figure 2.** Structure–activity/selectivity relationships derived from 3D-QSAR studies.

for **D1**, 105-fold selectivity for **D2**, 422-fold selectivity for **D3** vs 33-fold selectivity for **26**). Actually, more modifications on region II were done. Compounds with R<sub>2</sub> group such as CH<sub>3</sub>, CH<sub>2</sub>CH<sub>3</sub>, or CH<sub>2</sub>CH<sub>2</sub>N(CH<sub>3</sub>)<sub>2</sub> also had better ROCK2 inhibitory activity and ROCK2/PKA selectivity compared with **26** except the ROCK2/PKA selectivity while R<sub>2</sub> was CH<sub>2</sub>CH<sub>2</sub>N(CH<sub>3</sub>)<sub>2</sub>. So the models built in this work were effective for designing new highly potent and ROCK2/PKA selective ROCK inhibitors.

### 3. Conclusion

From the data set collected from urea-based ROCK inhibitors, 3D-QSAR models including CoMFA activity model, CoMFA

selectivity model, CoMSIA activity model, and CoMSIA selectivity model were set up, and the SAR/selectivity were obtained by analyzing the contour maps of CoMFA and CoMSIA models. Molecular docking further demonstrated that H-bonding interaction to residue Asp176 of ROCK2 was the key element for ROCK2/PKA selectivity. A 5 ns MD simulation certified the reliability of docking results. Finally, three new compounds were designed, synthesized, and biologically evaluated, and the potency data obtained from biochemical assays and prediction based on established 3Q-QSAR models were very similar and within the reasonable error range, which indicated that the molecular models were effective for designing highly potent and ROCK2/PKA selective ROCK inhibitors. The exploration of the ROCK1/ROCK2 isoform selectivity through

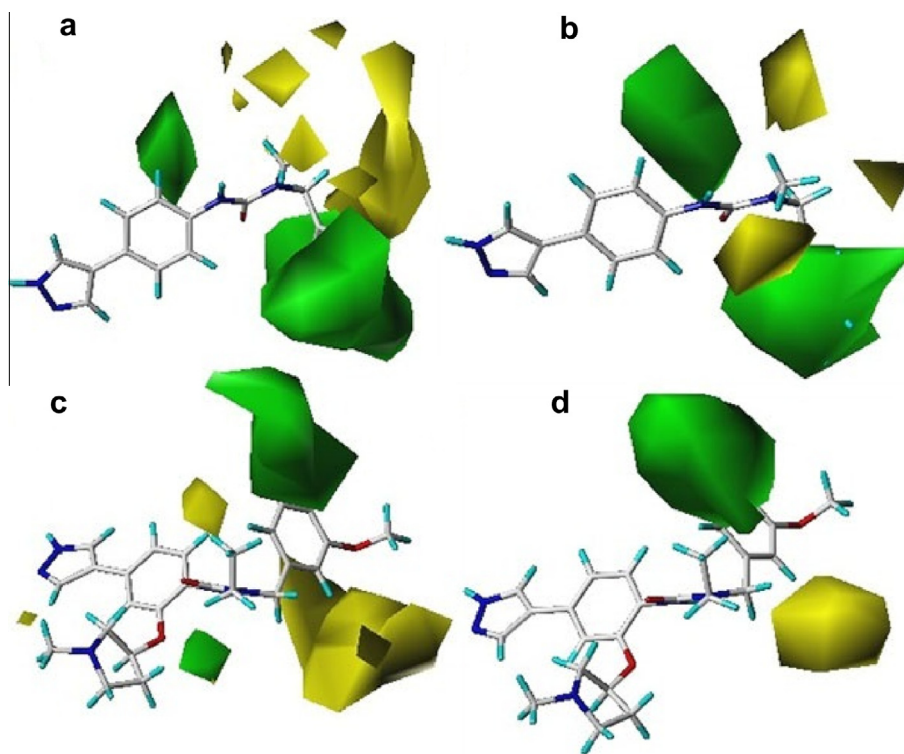


**Figure 3.** Contour maps of steric field: favored (green) and disfavored (yellow). (a) CoMFA activity model; (b) CoMSIA activity model; (c) CoMFA selectivity CoMFA model; (d) CoMSIA selectivity model.

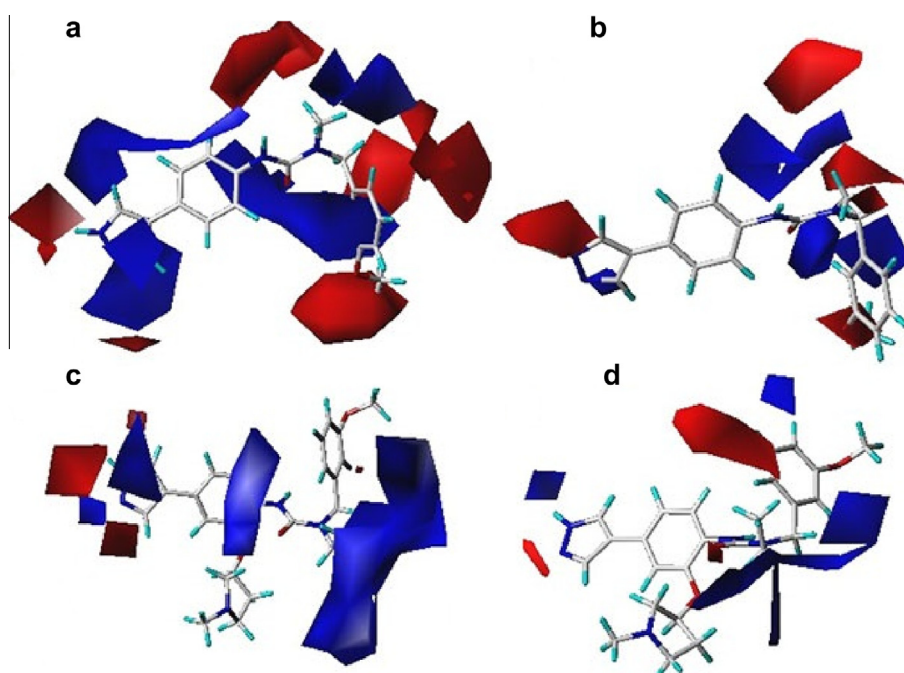


**Figure 4.** Contour maps of electrostatic field: electropositive (blue) and electronegative (red). (a) CoMFA activity model. (b) CoMSIA activity model. (c) CoMFA selectivity model. (d) CoMSIA selectivity model.

computer modeling is underway in our lab and will be published in due course.

#### 4. Experimental

Commercially available reagents and anhydrous solvents were used without further purification unless otherwise specified. Thin

layer chromatography (TLC) analyses were performed with pre-coated silica gel 60 F254. The mass spectra were recorded by LC/MS with Finnigan LCQ Advantage MAX spectrometer of Thermo Electron®. Flash chromatography was performed on prepacked columns of silica gel (230–400 Mesh, 40–63 µm) by CombiFlash® with EtOAc/hexane or MeOH/DCM as eluent. The preparative HPLC was performed on SunFire C18 OBD 10 µm (30 × 250 mm) with

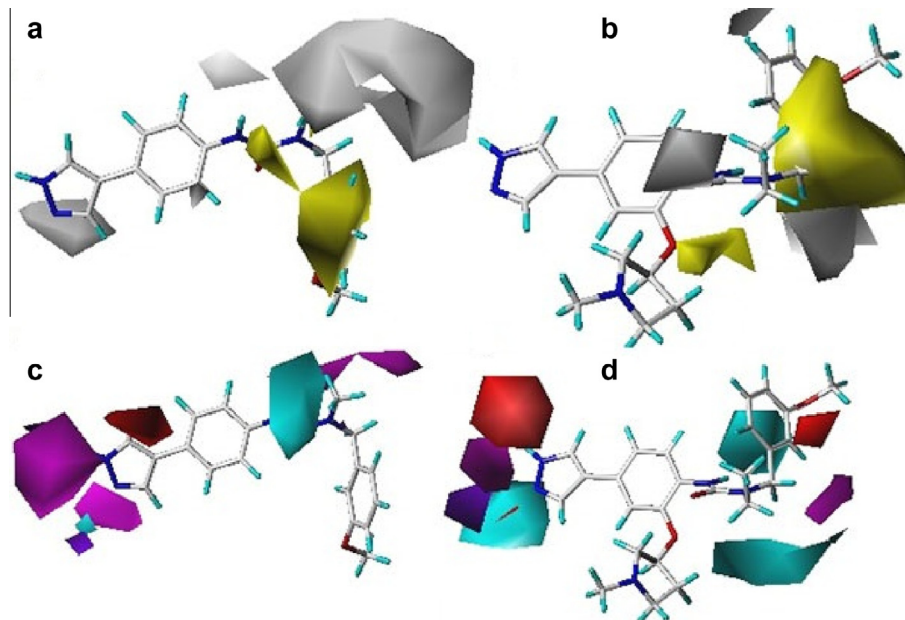


**Figure 5.** Contour maps of hydrophobic field and hydrogen bond donor/acceptor field. (a) Hydrophobic field of CoMSIA activity model. (b) Hydrophobic field of CoMSIA selectivity model. (c) Hydrogen bond donor/acceptor field of CoMSIA activity model. (d) Hydrogen bond donor/acceptor field of CoMSIA selectivity model. The yellow color shows the favored hydrophobic area, the white color shows the disfavored hydrophobic area. The cyan color shows the favored H-donor area, and the purple color represents the disfavored H-donor area. The magenta color shows the favored H-acceptor area, the red color shows the disfavored H-acceptor area.

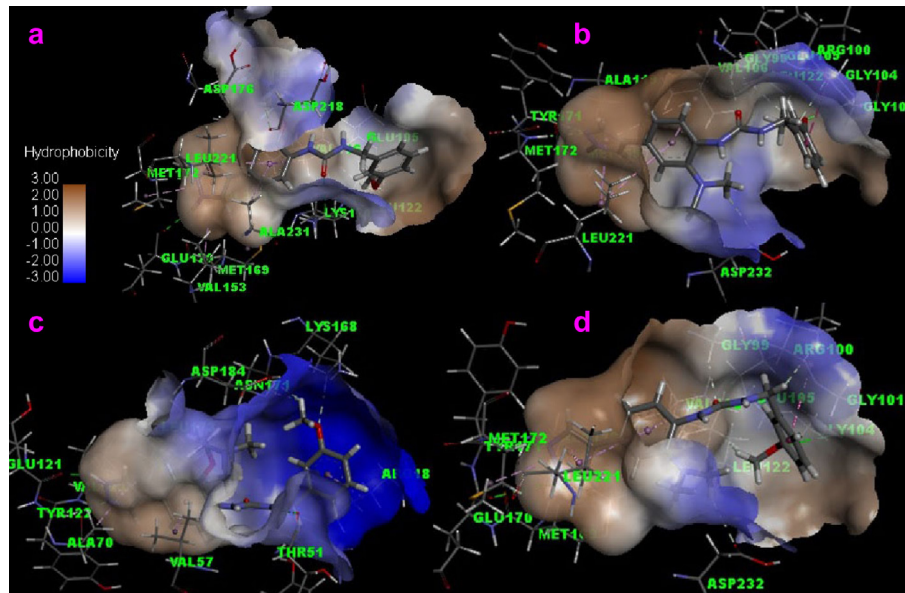


**Figure 6.** Docking results. (a) Docking of **16** into the binding site of ROCK2. (b) Docking of **12** into the binding site of ROCK2. (c) Docking of **16** into the binding site of PKA. (d) Docking of **12** into the binding site of PKA. Hydrogen bonds are shown as green dotted line.

$\text{CH}_3\text{CN} + 50\% \text{ MeOH}/\text{H}_2\text{O} + 0.1\% \text{TFA}$  as eluent to purify the targeted compounds. Analytic HPLC was performed on Agilent technologies 1200 series with  $\text{CH}_3\text{CN}$  (Solvent B)/ $\text{H}_2\text{O} + 0.9\% \text{ CH}_3\text{CN} + 0.1\% \text{TFA}$  (Solvent A) as eluent and the targeted products were detected by UV in the detection range of 215–310 nm. All compounds were determined to be >95% pure by this method. NMR spectra were recorded with a Bruker® 400 MHz spectrometer at ambient temperature with the residual solvent peaks as internal standards. The line positions of multiplets were given in ppm ( $\delta$ ) and the coupling constants ( $J$ ) were given in Hertz. The high-resolution mass spectra (HRMS, electrospray ionization) experiments were

performed with Thermo Finnigan orbitrap mass analyzer. Data were acquired in the positive ion mode at resolving power of 100,000 at  $m/z$  400. Calibration was performed with an external calibration mixture immediately prior to analysis.

#### 4.1. Synthetic procedures and structural characterization of D1, D2, and D3

To a mixture of 4-bromo-2-fluoro-nitrobenzene (1 mmol),  $\text{Cs}_2\text{CO}_3$  (3 mmol) in DMF (5 mL) was added *N,N,N'*-trimethyl-methanediamine or 2-dimethylamino-ethanethiol (1.05 mmol).

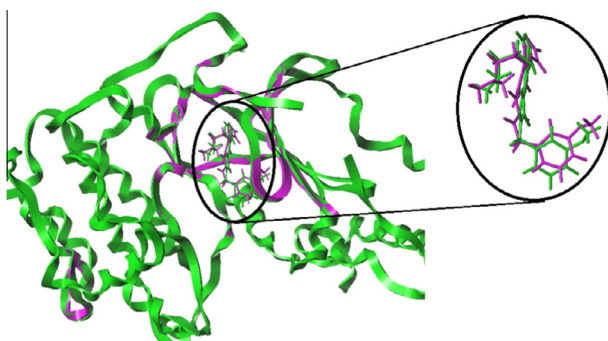


**Figure 7.** MD results of 4L6Q-**16** complex. The initial structure represent in magenta and the final structure represent in green.

After the completely conversion of the starting material detected by TLC, the mixture was quenched by water (2 mL) and extracted with EtOAc ( $3 \times 5$  mL). The combined organic extracts were washed with saturated brine, dried over anhydrous  $\text{Na}_2\text{SO}_4$ , concentrated under reduced pressure, and purified through silica gel to give substituted nitro benzene. The solution of substituted nitro benzene (1 mmol) in EtOAc (5 mL) was added tin chloride dehydrate (3 mmol). After stirring in room temperature until the complete disappearance of substituted nitro benzene detected by LC/MS, the mixture was quenched by water (2 mL) and extracted with EtOAc ( $3 \times 5$  mL). The combined organic extracts were washed with saturated brine, dried over anhydrous  $\text{Na}_2\text{SO}_4$ , concentrated under reduced pressure, and purified through silica gel to give aniline. Benzyl isocyanate (0.2 mmol) was added to a mixture of aniline (0.2 mmol), saturated  $\text{NaHCO}_3$  (0.5 mL) in DCM (1 mL) at  $0^\circ\text{C}$ . After stirring at room temperature for 0.5 h, the mixture was extracted with DCM ( $3 \times 5$  mL), dried over anhydrous  $\text{Na}_2\text{SO}_4$ , and concentrated in vacuo give crude bromide urea for next step without further purification.

To a solution of benzyl aldehyde (10 mmol) in methanol (20 mL) was added isopropylamine (10 mmol). After stirring at room temperature for 15 min, the solution was cooled to  $0^\circ\text{C}$  prior to the addition of sodium borohydride (5 mmol) portion wise. The resulting solution was stirred at room temperature for 1 h. After the addition of water (3 mL), methanol was removed under reduced pressure and the resulting aqueous phase was extracted with EtOAc ( $3 \times 15$  mL). The combined extracts were dried over anhydrous  $\text{Na}_2\text{SO}_4$  and concentrated in vacuo to give secondary benzyl amine. Then secondary benzyl amine (0.2 mmol) was added to the mixture of 1-bromo-4-isocyanatobenzene (0.2 mmol) in DCM at  $0^\circ\text{C}$ . After stirring at room temperature for 0.5 h, the mixture was extracted with DCM ( $3 \times 5$  mL), dried over anhydrous  $\text{Na}_2\text{SO}_4$ , and concentrated in vacuo give crude bromide urea for next step without further purification.

Finally, the 1*H*-pyrazoleboronic acid pinacol ester (0.3 mmol) and the crude bromide urea (0.2 mmol) were dissolved in degassed 5:1 dioxane/H<sub>2</sub>O. Pd(PPh<sub>3</sub>)<sub>4</sub> (0.02 mmol) and 2 M solution of  $\text{K}_2\text{CO}_3$  (0.6 mmol) were added sequentially under Argon and the mixture was heated at  $95^\circ\text{C}$  for 2 h. After cooling to room temperature, the mixture was diluted with water and extracted with ethyl acetate ( $3 \times 5$  mL). The organic layers were combined, dried over anhydrous  $\text{Na}_2\text{SO}_4$  and concentrated in vacuo. The residue was then purified by preparative HPLC to give the product **D1**, **D2**, and **D3** as white solid.

#### 4.1.1. 1-Benzyl-3-[2-(2-dimethylamino-ethylsulfanyl)-4-(1*H*-pyrazol-4-yl)-phenyl]-urea (**D1**)

Purity >99.9% (detected by UV at 215 nm, 230 nm, 254 nm, 280 nm, and 310 nm). <sup>1</sup>H NMR (DMSO-d<sub>6</sub>, 400 MHz) δ 9.59 (s, 1H), 8.12 (s, 1H), 8.04 (s, 2H), 8.00–7.98 (m, 1H), 7.71–7.70 (m, 1H), 7.54–7.51 (m, 2H), 7.38–7.26 (m, 5H), 4.33–4.31 (m, 2H), 3.20–3.18 (m, 4H), 2.77–2.76 (m, 6H). <sup>13</sup>C NMR (DMSO-d<sub>6</sub>, 100 MHz) δ 170.37, 158.39, 158.06, 154.32, 136.69, 134.74, 131.29, 128.47, 128.02, 127.92, 126.35, 124.21, 120.20, 114.97, 59.78, 49.67, 48.61, 39.37. LC/MS: (M+1) 396. HRMS calcd for  $\text{C}_{21}\text{H}_{26}\text{N}_5\text{OS} [\text{M}+\text{H}]^+$  396.1858, found: 396.1834.

#### 4.1.2. 1-Benzyl-3-[2-[2-dimethylamino-ethyl]-methyl-amino]-4-(1*H*-pyrazol-4-yl)-phenyl]-urea (**D2**)

Purity >99.9% (detected by UV at 215 nm, 230 nm, 254 nm, 280 nm, and 310 nm). <sup>1</sup>H NMR (DMSO-d<sub>6</sub>, 400 MHz) δ 9.33 (s, 2H), 8.26–8.13 (m, 2H), 8.01–7.88 (m, 2H), 7.44–7.43 (m, 1H), 7.37–7.24 (m, 7H), 4.32 (d,  $J = 5.6$  Hz, 2H), 3.28–3.21 (m, 4H), 2.74–2.73 (m, 6H), 2.59 (s, 3H). <sup>13</sup>C NMR (DMSO-d<sub>6</sub>, 100 MHz) δ 158.74, 155.39, 140.99, 140.23, 133.36, 128.30, 127.10, 126.73, 121.91, 121.09, 119.56, 118.50, 117.48, 114.57, 53.80, 49.57, 42.81, 42.74, 42.21. LC/MS (M+1): 393. HRMS calcd for  $\text{C}_{22}\text{H}_{29}\text{N}_6\text{O} [\text{M}+\text{H}]^+$  393.2403, found: 393.2422.

#### 4.1.3. 1-Benzyl-1-isopropyl-3-[4-(1*H*-pyrazol-4-yl)-phenyl]-urea (**D3**)

Purity >99.9% (detected by UV at 215 nm, 230 nm, 254 nm, 280 nm, and 310 nm). <sup>1</sup>H NMR (DMSO-d<sub>6</sub>, 400 MHz) δ 8.24 (s, 1H), 7.95 (s, 2H), 7.46–7.40 (m, 4H), 7.34–7.27 (m, 4H), 7.22–7.18 (m, 1H), 4.54 (s, 2H), 4.52–4.47 (m, 1H), 1.10 (s, 3H), 1.08 (s, 3H). <sup>13</sup>C NMR (DMSO-d<sub>6</sub>, 100 MHz) δ 163.46, 161.04, 156.02, 142.34, 137.85, 130.31, 126.96, 125.06, 123.14, 121.03, 120.11, 113.65, 49.33, 28.30, 8.94. LC/MS (M+1): 335. HRMS calcd for  $\text{C}_{20}\text{H}_{23}\text{N}_4\text{O} [\text{M}+\text{H}]^+$  335.1872, found: 335.1861.

#### 4.2. ROCK2 assay

Assays were performed using the STK2 kinase system from Cisbio. A 5  $\mu\text{L}$  mixture of a 1  $\mu\text{M}$  STK2 substrate and ATP (ROCK-

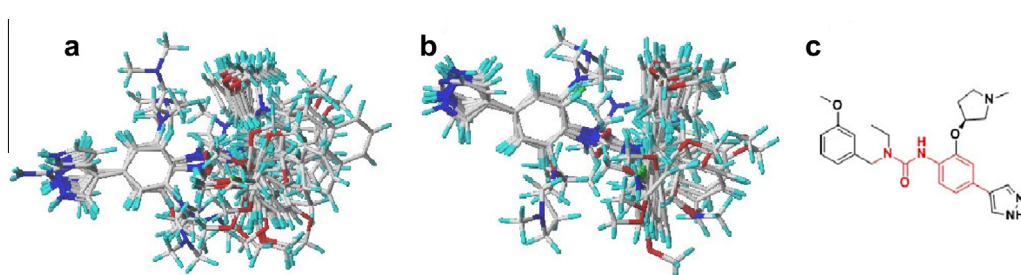
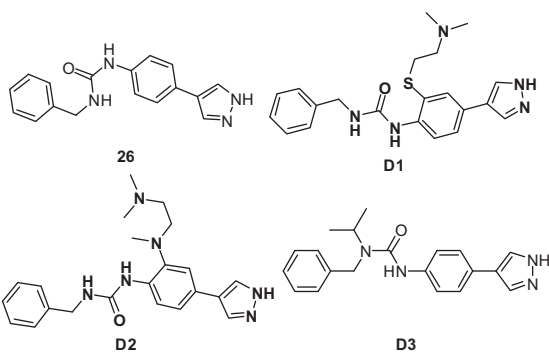


**Figure 8.** Alignment of training set. (a) Alignment of activity model with **42** as the template. (b) Alignment of selectivity model with **63** as the template. (c) Common substructure marked in red.

**Table 4**  
Activities of the new designed compounds



| Compd     | Experimental IC <sub>50</sub> (nM) |      | Pred. IC <sub>50</sub> (nM) by CoMFA |        | Pred. IC <sub>50</sub> (nM) by CoMSIA |        |
|-----------|------------------------------------|------|--------------------------------------|--------|---------------------------------------|--------|
|           | ROCK2                              | PKA  | ROCK2                                | PKA    | ROCK2                                 | PKA    |
| <b>26</b> | 18                                 | 590  | 26.2                                 | 8.7    | 18.4                                  | 5480   |
| <b>D1</b> | 5.6                                | 468  | 16.2                                 | 627    | 10.1                                  | 4027   |
| <b>D2</b> | 8.5                                | 894  | 10.1                                 | 466    | 5.4                                   | 2618   |
| <b>D3</b> | 8                                  | 3381 | 37.3                                 | 14,815 | 35.2                                  | 12,780 |

II: 20 μM in STK-buffer was added to the wells of the 384-well plate using a BioRAPTR FRD Workstation (Aurora Discovery, Carlsbad, CA). Twenty nanoliters of test compound was then dispensed using a 384-head offline Pintool system (GNF Systems, San Diego, CA). The reaction was started by adding either 5 μL of 0.5 nM ROCK-II in STK-buffer. After 4 h at rt the reaction was stopped by adding 10 μL of 1× antibody and 62.5 nM Sa-XL in Detection Buffer. After 1 h incubation at rt, the plates were read on the Viewlux in HTRF mode.

#### 4.3. PKA assay

A 5 μL mixture of 60 μM kemptide and 20 μM ATP in kinase buffer (50 mM HEPES pH 7.3, 10 mM MgCl<sub>2</sub>, 0.1% BSA, 2 mM DTT) was added to the wells using a BioRAPTR FRDTM Workstation (Aurora Discovery, Carlsbad, CA). Twenty nanoliters of test compound was then dispensed using a 384-head offline Pintool system (GNF Systems, San Diego, CA). The reaction was started by adding 5 μL of 0.5 nM PKA (Upstate #14-440) in kinase buffer (5 μL of kinase buffer was used for high wells). After 70 min incubation at rt, the reaction was stopped by adding 10 μL Kinase-Glo reagent and the plate was read after 10 min incubation at rt on the Viewlux in luminescence mode.

#### 4.4. Ligand preparation

3D structures of all compounds were constructed using the Sketch Molecule module and were fully minimized using the Tripos force field by the Powell gradient algorithm with Gasteiger-Hückel charges. The energy gradient termination criterion was set to 0.005 kcal/(mol Å) and the maximum iterations were set to 10,000. The alignment of training set compounds was shown in Figure 8a and b, and the common substructure marked in red was shown in Figure 8c.

#### 4.5. CoMFA and CoMSIA modeling

3D contour maps of CoMFA models and CoMSIA models were graphed using the Sybyl 2.0 program (Tripos, Inc., USA). The regression analysis was carried out using the partial least squares (PLS) method<sup>31,32</sup> and the final models were selected according to the statistical parameters.

#### 4.6. Molecular docking

Molecular docking was performed using the Surfflex-Dock module in Sybyl 2.0. Crystal structure of human ROCK2 (code: 4L6Q) and human PKA (code: 3POO) were downloaded from RCSB Protein Data Bank (<http://www.rcsb.org/pdb/home/home.do>). The ligands were docked in the corresponding protein's binding site by an empirical scoring function and a patented search engine in Surfflex-Dock. Before the docking process, the natural ligand was extracted and water molecules were removed from the crystal structure. Subsequently, the protein was prepared using Biopolymer module implemented in Sybyl. Then, a protomol was defined based on original ligand. By default, 20 conformations were generated for each molecule and the conformation with best score was chosen for further studies.

#### 4.7. Molecular dynamics (MD) simulations

MD simulations<sup>33–35</sup> was carried out in Sybyl 2.0 software. The conformation with best score was picked as initial conformation. Constant temperature (300 K) and volume were maintained with the time constant for a heat bath coupling of 100 fs. The time step of 1 fs was used to integrate the equations of motion, and the snapshot time was 100 fs and MD target was limited in the range of 3 Å with ligand as the core. The Boltzmann initial velocity was used to start the simulation. Other parameters were set by default in Sybyl 2.0.

#### Acknowledgements

The work was supported by Science and Technology Commission of Shanghai Municipality (Grant No. 12ZR1431100) and National Natural Science Foundation of China (No. 21172148). Support from Prof. Gang Zhao and Prof. Guanjun Wang was also greatly appreciated.

#### References and notes

- Nobes, C.; Hall, A. *Curr. Opin. Genet. Dev.* **1994**, *4*, 77.
- Chang, J.; Xie, M.; Shah, V. R.; Schneider, M. D.; Entman, M. L.; Wei, L.; Schwartz, R. J. *Proc. Natl. Acad. Sci. U.S.A.* **2006**, *103*, 14495.
- Re, D. P. D.; Miyamoto, S.; Brown, J. H. J. *Biol. Chem.* **2007**, *282*, 8069.
- Fukata, Y.; Kaibuchi, K.; Amano, M.; Kaibuchi, K. *Trends Pharmacol. Sci.* **2001**, *22*, 32.
- Micuda, S.; Rösel, D.; Ryska, A.; Bräbæk, J. *Curr. Cancer Drug Target* **2010**, *10*, 127.
- Tamura, M.; Nakao, H.; Yoshizaki, H.; Shiratsuchi, M.; Shigyo, H.; Yamada, H.; Ozawa, T.; Totsuka, J.; Hidaka, H. *Biochim. Biophys. Acta* **2005**, *1754*, 245.
- Pan, P. C.; Shen, M. Y.; Yu, H. D.; Li, Y. Y.; Li, D.; Hou, T. J. *Drug Discovery Today* **2013**, *18*, 1323.
- Qin, J.; Lei, B. L.; Xi, L. L.; Liu, H. X.; Yao, X. J. *Eur. J. Med. Chem.* **2010**, *45*, 2768.
- Wang, D. H.; Qu, W. L.; Shi, L. Q.; Wei, J. *Mol. Simul.* **2011**, *37*, 488.
- Shen, M. Y.; Zhou, S. Y.; Li, Y. Y.; Pan, P. C.; Zhang, L. L.; Hou, T. J. *Mol. BioSyst.* **2013**, *9*, 361.
- Davies, S. P.; Reddy, H.; Caivano, M.; Cohen, P. *Biochem. J.* **2000**, *351*, 95.
- Jacobs, M.; Hayakawa, K.; Swenson, L.; Bellon, S.; Fleming, M.; Taslimi, P.; Doran, J. *J. Biol. Chem.* **2006**, *281*, 260.
- Feng, Y. B.; Yin, Y.; Weiser, A.; Griffin, E.; Cameron, M. D.; Lin, L.; Ruiz, C.; Schürer, S. C.; Inoue, T.; Rao, P. V.; Schröter, T.; LoGrasso, P. V.; Feng, Y. B. *Med. Chem. Lett.* **2013**, *23*, 1592.
- Sessions, E. H.; Yin, Y.; Bannister, T. D.; Weiser, A.; Griffin, E.; Pocas, J.; Cameron, M. D.; Ruiz, C.; Lin, L.; Schürer, S. C.; Schröter, T.; LoGrasso, P.; Feng, Y. B. *Bioorg. Med. Chem. Lett.* **2008**, *18*, 6390.
- Yin, Y.; Lin, L.; Ruiz, C.; Cameron, M. D.; Pocas, J.; Grant, W.; Schröter, T.; Chen, W. M.; Duckett, D.; Schürer, S.; LoGrasso, P.; Feng, Y. B. *Bioorg. Med. Chem. Lett.* **2009**, *19*, 6686.
- Chen, Y. T.; Bannister, T. D.; Weiser, A.; Griffin, E.; Lin, L.; Ruiz, C.; Cameron, M. D.; Schürer, S.; Duckett, D.; Schröter, T.; LoGrasso, P.; Feng, Y. B. *Bioorg. Med. Chem. Lett.* **2008**, *18*, 6406.
- Chowdhury, S.; Sessions, E. H.; Pocas, J. R.; Grant, W.; Schröter, T.; Lin, L.; Ruiz, C.; Cameron, M. D.; Schürer, S.; LoGrasso, P.; Bannister, T. D.; Feng, Y. B. *Bioorg. Med. Chem. Lett.* **2011**, *21*, 7107.

19. Fang, X. G.; Chen, Y. T.; Sessions, E. H.; Chowdhury, S.; Vojkovsky, T.; Yin, Y.; Pocas, J. R.; Grant, W.; Schröter, T.; Lin, L.; Ruiz, C.; Cameron, M. D.; LoGrasso, P.; Bannister, T. D.; Feng, Y. B. *Bioorg. Med. Chem. Lett.* **2011**, *21*, 1844.
20. Yin, Y.; Lin, L.; Ruiz, C.; Khan, S.; Cameron, M. D.; Grant, W.; Pocas, J.; Eid, N.; Park, H. J.; Schröter, T.; LoGrasso, P. V.; Feng, Y. B. *J. Med. Chem.* **2013**, *56*, 3568.
21. Yin, Y.; Cameron, M. D.; Lin, L.; Khan, S.; Schröter, T.; Grant, W.; Pocas, J.; Chen, Y. T.; Pachori, S. A.; LoGrasso, P. V.; Feng, Y. B. *ACS Med. Chem. Lett.* **2010**, *1*, 175.
22. Cramer, R. D., III; Patterson, D. E.; Bunce, J. D. *J. Am. Chem. Soc.* **1988**, *110*, 5959.
23. Klebe, G.; Abraham, U.; Mietzner, T. *J. Med. Chem.* **1994**, *37*, 4130.
24. Böhm, M.; Stürzebecher, J.; Klebe, G. *J. Med. Chem.* **1999**, *42*, 458.
25. Wermuth, C. G. *The Practice of Medicinal Chemistry*, 2nd ed.; Elsevier: UK, 2003.
26. Golbraikh, A.; Tropsha, A. *J. Mol. Graph. Model.* **2002**, *20*, 269.
27. Patel, P. D.; Patel, M. R.; Kaushik-Basu, N.; Talele, T. T. *J. Chem. Inf. Model.* **2008**, *48*, 42.
28. Politis, A.; Durdagi, S.; Moutavelis-Minakakis, P.; Kokotos, G.; Mavromoustakos, T. *J. Mol. Graph. Model.* **2010**, *29*, 425.
29. Zhu, G. D.; Gong, J. C.; Gandhi, V. B.; Woods, K.; Luo, Y.; Liu, X. S.; Guan, R.; Klinghofer, V.; Johnson, E. F.; Stoll, V. S.; Mamo, M.; Li, Q.; Rosenberg, S. H.; Giranda, V. L. *Bioorg. Med. Chem.* **2007**, *15*, 2441.
30. Oh, K.; Mun, J.; Cho, J. E.; Lee, S.; Yi, K. Y.; Lim, C. J.; Lee, J. S.; Park, W. J.; Lee, B. H. *Comb. Chem. High Throughput Screening* **2013**, *16*, 37.
31. Takami, A.; Iwakubo, M.; Okada, Y.; Kawata, T.; Odai, H.; Takahashi, N.; Shindo, K.; Kimura, K.; Tagami, Y.; Miyake, M.; Fukushima, K.; Inagaki, M.; Amano, M.; Kaibuchi, K.; Iijima, H. *Bioorg. Med. Chem.* **2004**, *12*, 2115.
32. Stähle, L.; Wold, S. *J. Chemom.* **1987**, *1*, 185.
33. Kai, Z. P.; Ling, Y.; Liu, W. J.; Zhao, F.; Yang, X. L. *Biochim. Biophys. Acta* **2006**, *1764*, 70.
34. UI-HAQ, Z.; Khan, W.; Zia, S. R.; Iqbal, S. *J. Mol. Graph. Model.* **2012**, *36*, 48.
35. Yuan, M. G.; Luo, M. X.; Song, Y.; Xu, Q.; Wang, X. F.; Cao, Y.; Bu, X. Z.; Ren, Y. L.; Hu, X. P. *Bioorg. Med. Chem.* **2011**, *19*, 1189.